Unified Treatment for Dealing with Auxiliary Conditions in Blade Dynamics

A. Rosen,* R. G. Loewy,† and M. B. Mathew‡
Rensselaer Polytechnic Institute, Troy, New York 12181

Use of Lagrange multipliers is shown here to lead to a convenient method for the numerical analysis of blade dynamics in which a variety of auxiliary conditions may be imposed. General equations are derived that can deal with blades having virtually all of the possible combinations of boundary conditions. The method is combined with a generalized coordinates approach to obtain a unified and efficient formulation that is applicable to both linear and nonlinear situations. The different stages of the solution procedures are explained, and the method is demonstrated by calculating the natural frequencies of rotating and nonrotating blades having various boundary conditions at the root. The results of the present method are shown to agree very well with those from both transfer matrix analysis and exact analytical solution. Computational efficiencies available for design studies in which blade root flap, lag, and pitch springs and/or dampers are varied widely, for example, as used with a particular rotor blade, say, with substantial flap-pitch and flap-lag coupling, are a motivating factor in proposing this method. These aspects are also discussed.

I. Introduction

THE many different methods and approaches used for analyzing rotor blade dynamics may be found in the detailed list of references given, for example, in Refs. 1 and 2. Although many of these are methods of considerable generality, they often cannot be applied to special cases where the configuration of hub and hinge or special devices added to the blade require that auxiliary conditions be imposed on the mathematical description of blade behavior. There are a great variety of such conditions. Three are cited here as representative examples:

1) The so-called free-tip-rotor concept was introduced recently by Stroub et al.[3,4] In this case, the rotor blade "tip is free to pitch about an axis that is located forward of the blade cross-section aerodynamic center."[4] Thus, the tip has an aerodynamic tendency to weathervane into the tip's relative wind.

> Another device, called a "controller" applies a constant pitch moment to the tip, thus enabling the tip to weathervane about a prescribed null point that results in a finite pitch moment and, consequently, in a finite lift. Therefore, the free tip can generate a lift level that is nearly constant as it goes around the azimuth.[4]

Although the equations of motion for this blade are for the most part identical to those of blades without floating tips, there are special auxiliary conditions at the connection between the free tip and the rest of the blade that have to be satisfied at all times.

2) Outboard flapping hinge effects on the aerodynamic performance and dynamic response of two-bladed teetering rotors with a wide chord were studied experimentally by Weller and Lee.[5] They found that an outboard flapping hinge may reduce beamwise bending moments over a significant part of the blade radius, without significantly affecting the chordwise bending moments if its location is selected with proper consideration of rotor natural frequencies. The outboard flapping hinge also requires that special auxiliary conditions be imposed at the blade cross section where it is located.

3) Advanced rotor designs are continually increasing the variety of ways to attach blades to hubs. These include hinges with classical ball and roller or elastomeric bearings, coincident or separated; dampers about one or all axes; flex straps or beams; and kinematic or elastic coupling among the various blade root degrees of freedom. Although the equations of motion for the rest of the blade are not directly influenced by the method by which the blade is attached to the hub in most formulations, the boundary conditions at the root differ for each specific method of attachment. From a mathematical point of view, each case can be viewed as requiring different auxiliary conditions at the root.

The purpose of the present paper is to present a unified method for dealing with such auxiliary conditions. The method is unified in the sense that one formulation for rotor blade dynamic analysis will serve regardless of which or how many auxiliary conditions are added or how many exisiting auxiliary conditions are changed. The theoretical development proceeds by combining the method of Lagrange multipliers (Refs. 6–10, for example) with the generalized coordinate numerical model for predeformed beams recently derived by the authors.[11-15] Such a combination together with any other variational approach (finite elements, Rayleigh, Galerkin, etc.), may also give a similar unified approach. By choosing the proper set of generalized coordinates, however, it becomes possible with this methodology to treat virtually all of the possible boundary conditions (if they can be expressed mathematically) without either reformulation or providing new sets of shape functions for the generalized coordinates. It goes without saying that all of the associated recalculations of generalized stiffness, mass, and damping matrices are also avoided. In short, this formulation provides one set of basic equations that is applicable to all auxiliary constraint conditions and requires new numerical work in obtaining solutions for only a small part of the final equations as the auxiliary conditions are changed.

The use of this method will be demonstrated by calculating the natural frequencies and mode shapes for the free vibrations of rotating and nonrotating blades having various root boundary conditions. The accuracy of the method will be verified by comparing the results obtained here with those from other solutions for the same problems.

Received Sept. 25, 1989; revision received May 2, 1990; accepted for publication May 12, 1990.

*Senior Postdoctoral Fellow; on sabbatical leave from Technion—Israel Institute of Technology, Department of Aerospace Engineering, Haifa, Israel 32000. Member AIAA.

†Institute Professor. Fellow AIAA.

‡Postdoctoral Fellow; currently Senior Technical Specialist, Dynamics Boeing Helicopter Corporation, MS P 32-15, P.O. Box 16858, Philadelphia, PA 19142. Member AIAA.

II. Theoretical Background

A. Unconstrained Equations of Motion

The equations of motion for a rotor blade, obtained by using any variational approach including finite elements, finite differences, the Rayleigh-Ritz method, the Galerkin method, Lagrange's equations, and others, may, in general, be written as follows:

$$[A]\{\ddot{q}\} + [B]\{\dot{q}\} + [C]\{\dot{q}\} = \{f\} \tag{1}$$

where $\{q\}$ is the vector of unknowns representing the blade degrees of freedom. If there are N degrees of freedom associated with the mathematical model, then $\{q\}$ is of the Nth order. In general, $\{q\}$ is a function of time; an upper dot indicates differentiation with respect to time. The square matrices $[A]$, $[B]$, and $[C]$ are of order $N \times N$. It is clear that $\{f\}$ is a forcing vector, also of order N. In nonlinear cases, the matrices $[A]$, $[B]$, and $[C]$ and the vector $\{f\}$ may all be the functions of $\{q\}$ and $\{\dot{q}\}$.

B. Imposition of Auxiliary Conditions

Consider cases where, in addition to satisfying the equations of motion [Eq. (1)], there are N_λ auxiliary conditions that must be satisfied ($N_\lambda < N$). These conditions may be expressed in general terms as follows:

$$[R1]\{q\} + [R2]\{\dot{q}\} = \{r\} \tag{2}$$

Here, $[R1]$ and $[R2]$ are $N_\lambda \times N$ rectangular matrices, and $\{r\}$ is a vector of order N_λ. An example of a situation leading to a matrix of the $[R_1]$ variety would be a hinged, multibody system whose equations of motion are given by Eq. (1) and whose dynamic characteristics are to be determined with springs added about the hinges. Hinge moments equal to such spring rates times the angular displacements about the hinges (in terms of the generalized coordinates q) would be considered constraints in this approach and would lead to $[R_1]$-type relations. If the influence of viscous dampers were to be added as constraints, they would lead to $[R_2]$-type relations, on the same basis. Examples of other kinds of constraints are given in Sec. IV of this paper.

The auxiliary conditions expressed by Eq. (2) may be nonlinear in the sense that $[R_1]$, $[R_2]$, and/or $\{r\}$ can be functions of $\{q\}$ and $\{\dot{q}\}$. Following the example just cited, $[R_2]$ relations of a nonlinear type would be required if hydraulic damping, i.e., proportional to velocities squared, were to be represented.

A straightforward way of solving a problem in such a constraint formulation is to eliminate N_λ of the N elements of the vector $\{q\}$ as functions of the (N-N_λ) other variables by using Eq. (2). This approach reduces the original N equations to (N-N_λ) equations, but it requires reformulation for every change in the auxiliary, i.e., constraint, conditions [Eq. (2)]. In the following Secs. C and D, an approach is outlined that eliminates the need for reformulation and, in addition, requires new input in a numerical solution only for the parts of the calculation directly attributable to the constraints (matrices $[R_1]$, $[R_2]$, and $\{v\}$) and not the basic system acted on by the constraints (matrices $[A]$, $[B]$, $[C]$, and $\{f\}$).

C. Use of Lagrange Multipliers

The method of Lagrange multipliers provides a useful alternative approach to the straightforward elimination of N_λ variables. A general description of this well-known method may be found in many references (e.g., 6–10). Only a brief summary and application for our purposes is given here.

The Lagrangian of any system can be written in the following general form:

$$L(\dot{q}, q) = T(\dot{q}, q) - V(q) + \sum_{j=1}^{N_\lambda} \lambda_j C_j(\dot{q}, q) \tag{3}$$

where T and V are the kinetic and potential energies of the entire system, respectively, and the terms $C_j(\dot{q},q)$ represent the N_λ constraints, which have been defined previously by Eq. (2). The factors λ_j are N_λ Lagrange multipliers; they can be looked on as N_λ new unknowns. In general, λ_i are functions of time.

The system of ($N + N_\lambda$) equations of motion is given by applying the followng Lagrange equations:

$$\frac{\mathrm{d}}{\mathrm{d}1}\left(\frac{\partial L}{\partial \dot{q}_j}\right) - \frac{\partial L}{\partial q_j} = Q_j \qquad 1 \le j \le N \tag{4a}$$

$$C_i(\dot{q}, q) = 0 \qquad 1 \le i \le N_\lambda \tag{4b}$$

where the terms Q_j are the generalized forces associated with the unknown generalized coordinates q_j.

Substituting Eq. (3) into Eq. (4a) results in the following system of equations:

$$[A1]\{\ddot{q}\} + [B]\{\dot{q}\} + [C]\{q\} + [R3]\{\lambda\} + [R4]\{\dot{\lambda}\} = \{f\} \tag{5a}$$

$$[R1]\{q\} + [R2]\{\dot{q}\} = \{r\} \tag{5b}$$

where $\{\lambda\}$ is the vector of Lagrange multipliers. The matrices $[R3]$ and $[R4]$ result from substituting the summation that appears in Eq. (3) into the second and first terms on the left side of Eq. (4a), respectively. The matrices $[B]$, $[C]$, $[R1]$, and $[R2]$ and the vector $\{f\}$ have been defined following Eqs. (1) and (2). The matrix $[A1]$ will differ from the matrix $[A]$ that appears in Eq. (1) only if the constraints include products of the time derivatives of the unknowns, namely products of $\dot{q}_j$. Since practical constraints only rarely contain products of these time derivatives, in most cases, $[A1]$ will be identical to $[A]$.

Equations (5a) and (5b) represent ($N + N_\lambda$) coupled equations in the unknowns $\{q\}$ and $\{\lambda\}$. Thus, the number of both equations and unknowns has been increased by N_λ. As noted earlier, however, in return for this increase in order, the following advantages are obtained. With the proper choice of generalized coordinates, as described in Sec. C, the numerical values in the matrices $[A]$, $[B]$, and $[C]$ and vector $\{f\}$ do not change for a given system as a result of changes in auxiliary conditions; only the matrices $[R1]$, $[R2]$, $[R3]$, $[R4]$, and $[R5]$ and the vector $\{r\}$ are influenced by constraint changes. To the authors' knowledge, this is the only means of achieving the associated computational efficiency in structural dynamic analyses where the effects of a substantial number of variations of constraint parameters are to be studied. In addition, the complexity associated with eliminating N_λ variables in reformulations as the kind of constraints are changed, using Eq. (2), is avoided.

A convenient method for solving the system defined by Eqs. (5a) and (5b) is to define a state vector $\{X\}$, of order ($2N + N_\lambda$), as follows:

$$\{X\}^t = \langle \{\dot{q}\}^t, \{q\}^t, \{\lambda\}^t \rangle \tag{6}$$

Note that here and in the rest of this paper the symbology $\langle\ \rangle$ denotes a row matrix.

The system of equations [Eqs. (3a) and (3b)] then becomes

$$\begin{bmatrix} [A1] & 0 & [R4] \\ 0 & [I] & 0 \\ 0 & 0 & 0 \end{bmatrix} \{\dot{X}\} + \begin{bmatrix} [B] & [C] & [R3] \\ [-I] & 0 & 0 \\ [R2] & [R1] & 0 \end{bmatrix}$$

$$\{X\} = \begin{Bmatrix} \{f\} \\ 0 \\ \{r\} \end{Bmatrix} \tag{7}$$

Here $[I]$ is an $N \times N$ identity matrix.

D. Solution of the Constrained Equations

Solution of Eq. (7) yields the behavior of the blade under the influence of the auxiliary conditions. This system of equations can be solved easily for eigenvalues and vectors (see the examples of Sec. IV) or for periodic response in terms of a series of harmonic functions. On the other hand, the fact that the matrix of coefficients of $\{\dot{X}\}$ is singular can cause difficulties if attempts are made to use other solution techniques. Attempts to bring Eq. (7) to the form

$$\{\dot{X}\} = f(X,t) \tag{8}$$

in preparation for solution by a standard numerical integration with time scheme, for example, may encounter such problems. These problems are inherent to dynamic problems associated with using Lagrange multipliers, and there are various efficient and easy-to-use techniques to overcome them. One approach is to reduce the order of the vector of state variables by eliminating N_λ of the q_j unknowns from the state vector. Note that, at this point, this is a numerical procedure, in contrast to the formulation approach discussed in the final paragraph of Sec. B. Once this is done, then the $2N$ upper equations of the system of Eq. (7) can be integrated with time, usually without problems. The last N_λ equations can be used to solve for the N_λ unknowns that have been eliminated at any point in time, as required. This is a straightforward numerical procedure that can be done automatically; it has been used by the authors and has proved to be simple and efficient.

This section has concentrated on a discussion of the equations for the general case, incorporating any kind of auxiliary conditions and without being specific as to a recommended method of solution. In the next section, this Lagrange multiplier formulation is combined with a generalized coordinates technique to yield a unified mathematical model for rotor blades incorporating virtually all possible boundary conditions at the root, as may be provided by using various techniques of attaching blade to hub and controlling its pitch.

III. Derivation of a Unified Rotor Blade Model with Various Root Boundary Conditions

A. Introducing Generalized Coordinates and the Principal Curvature Transformation

Almost any theoretical dynamic model that has been obtained using a variational principle can be subjected to the method of Lagrange multipliers. A relatively new method[11-15] derived from variational principles will be used here. It combines a so-called principal curvature transformation, velocity component transformation, and a generalized coordinates technique and has been shown[12-15] to offer an efficient tool for solving a variety of rotor blade dynamics problems. A brief description of the method, which is necessary for the derivations in the rest of the paper, follows. The interested reader may find more detailed descriptions in Refs. 11-15.

The method deals with a blade having a straight elastic axis. Coordinate axes are chosen such that x lies along the blade axis positive outward, whereas y and z are cross-sectional coordinates in the lead-lag and flap directions, respectively. The components of the displacements of each point along the elastic axis in the x, y, and z directions are u, v, and w, respectively. Rotations of the cross section about the elastic axis are defined by an angle ϕ. Adopting the inextensionality assumption,[11] u becomes a function of v and w along the blade and the axial displacement (in the x direction), if any, at the root of the blade u_o. The displacement components and torsional rotations along the blade length are described by the following series of generalized coordinates:

$$u = u_o + \sum_{n=1}^{Nu} q_{u(n)} FU_{(n)} \tag{9a}$$

$$v = \sum_{j=1}^{Nv} q_{v(j)} FV_{(j)} \tag{9b}$$

$$w = \sum_{k=1}^{Nw} q_{w(k)} FW_{(k)} \tag{9c}$$

$$\phi = \sum_{l=1}^{N\phi} q_{\phi(l)} F_{\phi(l)} \tag{9d}$$

Here, $q_{v(j)}$, $q_{w(k)}$, and $q_{\phi(l)}$ are the generalized coordinates, functions of time. As mentioned earlier, each $q_{u(n)}$ is a known function of $q_{v(j)}$ and $q_{w(k)}$. The shape functions $FU_{(n)}$, $FV_{(j)}$, $FW_{(k)}$, and $F\phi_{(l)}$ are presumed known for each generalized coordinate. The vector of unknown general coordinates becomes

$$\{q\}^t = \langle q_{v(1)}, \ldots, q_{v(j)}, \ldots, q_{v(Nv)}, q_{w(1)}, \ldots, q_{w(k)}, \ldots, q_{w(Nw)}, q_{\phi(1)}, \ldots, q_{\phi(l)}, \ldots, q_{\phi(N\phi)} \rangle \tag{10}$$

The components of the cross-sectional resultant moments are the torsional component M_x (perpendicular to the cross section) and the bending moment components M_η and M_ζ in the principal directions of the cross section. These moment components are given by

$$M\zeta = (EI_{\eta\eta}) v_{e,xx} \tag{11a}$$

$$M_\eta = (EI_{\zeta\zeta}) w_{e,xx} \tag{11b}$$

$$M_x = (GJ) \phi_{e,x} \tag{11c}$$

where $(EI_{\eta\eta})$ and $(EI_{\zeta\zeta})$ are the principal components of the cross-sectional bending stiffness and (GJ) is the torsional stiffness. The particular combinations of space derivatives of physical deformations defined as $v_{e,xx}$, $w_{e,xx}$, and $\phi_{e,x}$ are the principal curvature and twist components. Generalized coordinates are also used to describe these quantities, as follows:

$$v_{e,xx} = \sum_{j=1}^{Nve} q_{ve(j)} FV''_{e(j)} \tag{12a}$$

$$w_{e,xx} = \sum_{k=1}^{Nwe} q_{we(k)} FW''_{e(k)} \tag{12b}$$

$$\phi_{e,x} = \sum_{l=1}^{N\phi e} q_{\phi e(l)} F\phi'_{e(l)} \tag{12c}$$

An upper prime here indicates differentiation with respect to x. $FV''_{e(j)}$, $FW''_{e(k)}$, and $F\phi'_{e(l)}$ are shape functions corresponding to the generalized coordinates of the principal curvature and elastic twist distributions $q_{ve(j)}$, $q_{we(k)}$, and $q_{\phi e(l)}$.

Just as for the vector $\{q\}$, a vector $\{q_e\}$of order N_e is defined as

$$\{q_e\}^t = \langle q_{ve(1)}, \ldots, q_{ve(j)}, \ldots, q_{ve(N_v)}; q_{we(1)}, \ldots, q_{we(k)}, \ldots, q_{we(N_{we})}; q_{\phi e(1)}, \ldots, q_{\phi e(l)}, \ldots, q_{\phi e(N_{\phi e})} \rangle \quad (13a)$$

$$N_e = N_{ve} + N_{we} + N_{\phi e} \quad (13b)$$

The definition of principal curvatures based on equivalent strain energy allows writing the relation [see Eq. (28) of Ref. 11]:

$$\{q_e\} = [D1]^{-1}([D2] + [D3])\{q\} \quad (14)$$

The matrices $[D1]$ and $[D2]$ have constant terms, whereas the matrix $[D3]$ is a function of $\{q\}$ and thus contains nonlinear contributions. The matrix $[D1]$ is of order $N_e \times N_e$, whereas $[D2]$ and $[D3]$ are of order $N_e \times N$. All are derived and defined in Ref. 11.

From Eqs. (9), (11), (12), and (14), it is clear that it should be possible to describe the displacement, rotation-linear velocity, angular velocity, or resultant moment (at any point along the blade) as a function of $\{q\}$ and $\{\dot{q}\}$. Thus, it is possible to express any auxiliary condition associated with these variables in the form shown in Eq. (2). Moreover, if the auxiliary conditions involve components of the cross-sectional resultant transverse shearing force, these components can also be described as functions of $\{q\}$. Such expressions have not been presented here, and resultant shearing forces will not be accounted for in the present examples.

The equations of motion of a rotor blade were obtained in Ref. 14 by writing the Lagrangian of the system and applying Lagrange's equations. This resulted in equations in the form shown in Eq. (1) [see Eq. (56) of Ref. 11].

B. Applied Loads at the Blade Root

Since one of the purposes here is to separate the boundary conditions at the blade root from the rest of the problem, it is convenient to separate the loading vector $\{f\}$ of Eq. (1) into two parts:

$$\{f\} = \{\overset{*}{f}\} + \{f_r\} \quad (15)$$

$\{f_r\}$ presents loads that are acting at the root, whereas $\{\overset{*}{f}\}$ loads presents the rest of the loads along the blade.

The root forces $\{f_r\}$may include loads that are functions of the blade deformations. These may be either passive loads resulting, for example, from flexibility or friction at the root, or active loads applied by a feedback control system that uses the blade deformations as an input.

It is, therefore, convenient to express $\{f_r\}$ as

$$\{f_r\} = [A_r]\{q\} + [B_r]\{\dot{q}\} + [C_r]\{q\} + \{d\} \quad (16)$$

where $[A_r]$, $[B_r]$, and $[C_r]$ are Nth order square matrices. Their elements can be determined, for example, by using virtual work principles.[16,17]

In the general, nonlinear case, these matrices may be functions of $\{q\}$and $\{\dot{q}\}$; $\{d\}$, however, is not a function of $\{q\}$ or $\{\dot{q}\}$.

Substitution of Eq. (16) into Eq. (1) yields

$$[\tilde{A}]\{q\} + [\tilde{B}]\{\dot{q}\} + [\tilde{C}]\{q\} = \{\tilde{f}\} \quad (17)$$

where

$$[\tilde{A}] = [A] - [A_r], \qquad [\tilde{B}] = [B] - [B_r] \quad (18a)$$

$$[\tilde{C}] = [C] - [C_r] \qquad \{\tilde{f}\} = \{\overset{*}{f}\} + \{d\} \quad (18b)$$

Equation (17) is simply the system equation of motion, Eq. (1), with those loads due to root motions incorporated into dependent variable terms. The method of Lagrange multipliers may be applied to the solution of Eq. (17) in the manner described earlier if, for example, there are kinematic constraints to be accounted for. Force and moment constraints at the root can be imposed as discussed here or through the Lagrange multiplier techniques as done later in this paper. Using Eq. (17) when representing applied loads rather than Eq. (1) has the same advantage that using Lagrange multipliers for constraints has; namely, that changes in loads at the root will be confined to changes in $[A_r]$, $[B_r]$, $[C_r]$, and $\{d\}$, whereas the rest of the elements, which represent the majority of the blade, will not be affected.

C. Definition of Particular Generalized Coordinates

Generalized coordinate methods are widely used in blade analysis because of their efficiency and the physical insight they usually provide. Unfortunately, a change of the boundary conditions (e.g., at the root) usually requires defining a new set of generalized coordinates and, thus, a time-consuming, complete recalculation of the whole problem. If a case should be encountered for which boundary conditions are continuously changing, it would seem that the entire advantage of using the generalized coordinates method would be lost. It is possible, however, to choose a special class of generalized coordinates, uninfluenced by root conditions and, thus, providing an efficient unified mathematical model, appropriate for virtually any combination of root boundary conditions. These general coordinates are as follows:

$$FV_{(1)} = FW_{(1)} = F\phi_{(1)} = 1 \quad (19a)$$

$$FV_{(2)} = FW_{(2)} = x \quad (19b)$$

$$FV_{(j)}(x=0) = FV'_{(j)}(x=0) = 0 \qquad \text{for } j \geq 3 \quad (19c)$$

$$FW_{(k)}(x=0) = FW'_{(k)}(x=0) = 0 \qquad \text{for } k \geq 3 \quad (19d)$$

$$F\phi_{(l)}(x=0) = 0 \qquad \text{for } l \geq 2 \quad (19e)$$

that is, j, $k < 3$ are normalized rigid body modes and j, $k \geq 3$ and $l \geq 2$ are cantilevered modes. The series that describes the axial displacement u is chosen identical to the series describing either v or w, where the first term in the series is u_o.

The advantages of this choice of generalized coordinates are as follows:

1) Whatever number of generalized coordinates are used, only u_o, $q_{v(1)}$, $q_{u(2)}$, $q_{w(1)}$, $q_{w(2)}$, and $q_{\phi(1)}$ affect motions at the root. This results in a significant simplification and increase in flexibility in dealing with different boundary conditions at the root.

2) The strain energy of the blade is not affected by $q_{v(1)}$, $q_{v(2)}$, $q_{w(1)}$, $q_{w(2)}$, and $q_{\phi(1)}$. In fact, from a strain energy point of view, one will always deal with the case of a fully hingeless (clamped) blade. The terms $q_{v(1)}$, $q_{v(2)}$, $q_{w(1)}$, $q_{w(2)}$, and $q_{\phi(1)}$ represent the root degrees of freedom whose degree of constraint often change in the evolution of a design. Thus, following the introduction of generalized coordinates, the structural parts of the theoretical model are not influenced by changes in boundary conditions.

D. Solution Procedure

The steps involved in solving a blade problem with this formulation are straightforward. Using the method presented in Refs. 11 and 14, choosing the generalized coordinates according to Eqs. (19a–c), and neglecting (for the moment) any loads that act at the blade root (or any other influences of boundary conditions at the root), the matrices $[A]$, $[B]$, and $[C]$ and the vector $\{\overset{*}{f}\}$ are calculated. Note that this part of the calculation will not be repeated so long as the inertial/

structural/geometrical properties of the blade are not changed. If the boundary conditions involve loads at the root, the matrices $[A_r]$, $[B_r]$, and $[C_r]$ and the vector $\{d\}$ are assembled according to Eq. (16) and the matrices $[A]$, $[B]$, and $[C]$ and the vector $\{f\}$ are calculated according to Eqs. (18). The matrices $[R1]$ and $[R2]$ and the vector $\{r\}$ given in Eq. (2) are derived for the specific boundary conditions of interest. Note that what is done here must be compatible with and not duplicative of what is done in calculating $[\tilde{A}]$, $[\tilde{B}]$, $[\tilde{C}]$, and $\{\tilde{f}\}$. Each boundary condition relation is multiplied by a different (and undetermined) Lagrange multiplier and all are added to the system Lagrangian. The matrices $[R3]$, $[R4]$, and $[R5]$ then result from any standard dynamic equation derivation technique (see, e.g., Ref. 10). Equation (7) is assembled by replacing $[B]$, $[C]$, and $\{f\}$ with $[\tilde{B}]$, $[\tilde{C}]$, and $\{\tilde{f}\}$, respectively, and $[A]$, or $[A1]$ if necessary, by $[\tilde{A}]$. Solution of these equations will provide time response, stability, or eigenvalues for the system.

IV. Sample Applications: Free Blade Vibrations in a Vacuum

A. Description of the Blade Model

All of the examples in this section deal with one blade design, but with different root boundary conditions. In focusing on the treatment of the boundary conditions, a simple blade model has been chosen; it has uniform properties, zero pretwist, and the cross-sectional center of mass is located on the elastic axis. The principal directions of the blade cross sections coincide with the lead-lag and flap directions. It is assumed that the free vibrations are small, in a vacuum, and take place about a state in which the blade is: 1) undeformed except for small axial elongation; and 2) perpendicular to the shaft. The blade properties that are assumed are the following: flapping stiffness $(EI_{\zeta\zeta}) = 8.3225 \cdot 10^4$ N-m^2; lead-lag stiffness $(EI_{\eta\eta}) = 1.7506 \cdot 10^6$ N-m^2; torsional stiffness $(GJ) = 7.1746 \cdot 10^4$ N-m^2; mass per unit length $(m) = 14.341$ kg/m; cross-sectional mass moments of inertia $(MI_{yy}) = 0.17682$ kg-m and $(MI_{zz}) = 0.00842$ kg-m; and length $(L) = 7.4676$ m. Unless otherwise stated, the blade rotates at a speed of 286 rpm.

The calculations were performed with five generalized coordinates in each of the series [Eqs. (9)], not including transverse displacement at the root. In these cases,

$$v(x=0) = w(x=0) = 0 \tag{20}$$

This equation indicates that the first term in the v, w series (representing this displacement) can be dropped, and this was done in the actual calculation to save computing time. Nevertheless, derivations in the following section are written as if these generalized coordinates $[FV_{(1)}, FW_{(1)}]$ do exist in the series, so as to make them potentially more useful.

B. Case of δ_3 Hinge with Zero Offset

Cases where there is kinematic coupling between flap and pitch appear many times in the literature. A schematic description of such a so-called δ_3 hinge is shown in Fig. 1 and is used here to both illustrate and confirm the method. The offset f_x is taken equal to zero. For free vibrations about a state of zero predeformation, the root boundary conditions are

$$v = w = v_{,x} = 0 \tag{21a}$$

$$w_{,x} \tan\delta_3 - \phi = 0 \tag{21b}$$

$$M_\eta - M_x \tan\delta_3 = 0 \tag{21c}$$

In addition to satisfying Eq. (20) by taking $q_{v(1)}$ and $q_{w(1)}$ equal to zero, we will satisfy the third of Eqs. (21a) by also taking $q_{v(2)}$ equal to zero. As a reminder as to the mode shapes thus eliminated, see Eqs. (19a) and (19b). Some computer time will be conserved as well. Considering all of the remaining boundary conditions, the matrix $[R1]$ in Eqs. (2) and (3b) is of order $5 \times N$, defined as follows:

$$[R1] = \begin{bmatrix} \langle M1 \rangle \\ \langle M2 \rangle \\ \langle M3 \rangle \\ \langle M4 \rangle \\ \langle M5 \rangle \end{bmatrix} \tag{22}$$

where $\langle Mi \rangle$ $(i = 1\text{–}5)$ are the N-dimensional row vectors given in the following [see Eqs. (9) and (11–14)]:

$$\langle M1 \rangle = \langle 1, (N_v + N_w + N_\phi - 1) \text{ zeros} \rangle \tag{23a}$$

$$\langle M2 \rangle = \langle N_v \text{zeros}, 1, (N_w + N_\phi - 1) \text{ zeros} \rangle \tag{23b}$$

$$\langle M3 \rangle = \langle 0, 1, (N_v + N_w + N_\phi - 2) \text{ zeros} \rangle \tag{23c}$$

$$\langle M4 \rangle = \langle (N_v + 1) \text{ zeros}, -\tan\delta_3, (N_w - 2) \text{ zeros}, 1, (N_\phi - 1) \text{ zeros} \rangle \tag{23d}$$

$$\langle M5 \rangle = \langle M6 \rangle [D1]^{-1}[D2] \tag{23e}$$

Equation (23e) reflects the fact that $[D3]$ is zero in the linear case. The matrix $\langle M6 \rangle$ is a row vector of order N_e, defined by

$$\begin{aligned} \langle M6 \rangle = \langle & N_{ve}\text{zeros}, (EI_{\zeta\zeta})FW''_{e(1)}(x=0), \ldots, \\ & (EI_{\zeta\zeta})FW''_{e(k)}(x=0), \ldots, (EI_{\zeta\zeta})FW_{e(N_{we})}(x=0); \\ & \tan\delta_3 \, (GJ)\phi_{e(2)}(x=0), \ldots, \tan\delta_3 (GJ)\phi'_{e(l)} \\ & (x=0), \ldots, \tan\delta_3 (GJ)\phi_{e(N_{\phi e})}(x=0) \rangle \end{aligned} \tag{24}$$

Equation (23a) corresponds to the first condition in Eq. (21a); Eq. (23b) to the second; and Eq. (23c) to the third. Equation (23d) corresponds to Eq. (21b). Equations (23e) and (24) correspond to Eq. (21c) with the insertion of Eqs. (11) and (12).

Since this is a linear case ($[R1]$ and $[R2]$ are not functions of $\{q\}$ or $\{\dot{q}\}$), then it is easy to show (see, e.g., Ref. 10) that

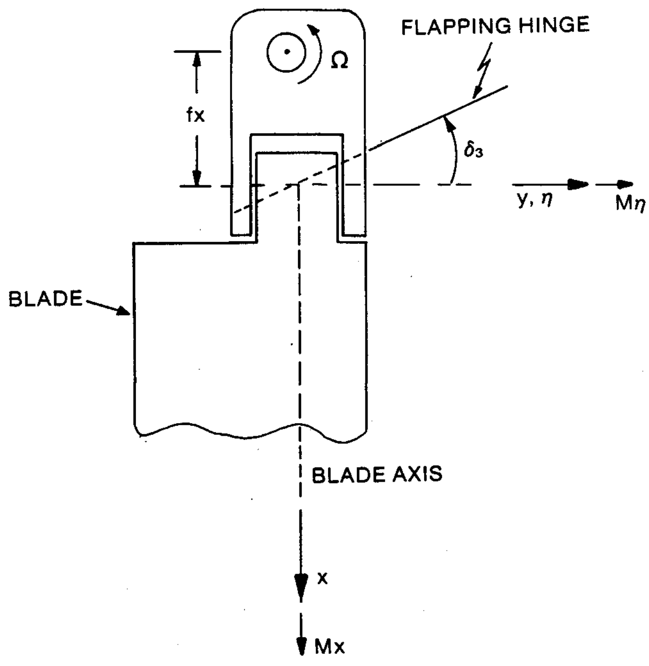

Fig. 1 Schematic description of a δ_3 hinge.

$$[R3] = [R1]^t \quad (25a)$$

$$[R4] = [R2]^t \quad (25b)$$

$$[R5] = 0 \quad (25c)$$

In this case, furthermore, since no boundary conditions involve the velocities associated with root motion,

$$[R2] = 0 \quad (26)$$

Since free vibrations are of interest here (about a nondeformed state), it is assumed that the state vector [see Eq. (6)] can be expressed as

$$\{X\} = \{X_o\}e^{\bar{\omega}t} \quad (27)$$

Where $\bar{\omega}$ is a complex frequency and $\{X_o\}$is a complex vector of order $(2N + N_\lambda)$, representing the contribution of individual mode shapes to the resulting motion. Substituting Eq. (27) into the equations of motion [Eq. (7)] to the following eigenvalue formulation:

$$\left\{ \bar{\omega} \begin{bmatrix} [\tilde{A}] & 0 & [R4] \\ 0 & [I] & 0 \\ 0 & 0 & 0 \end{bmatrix} + \begin{bmatrix} [\tilde{B}] & [\tilde{C}] & [R3] \\ [-I] & 0 & 0 \\ [R2] & [R1] & 0 \end{bmatrix} \right\}$$

$$\times \{X_o\} = 0 \quad (28)$$

In this case, [˜] = [ ], and the expressions for the dynamic equation matrices $[A]$, $[B]$, and $[C]$ are given in Eq. (59) of Ref. 14. Solving this equation yields the frequencies and mode shapes.

In Fig. 2, the variations of the frequencies of the first three flap/torsion modes are presented as functions of the angle δ_3 for the sample blade. The lead-lag modes are uncoupled and are not influenced by δ_3. For comparison purposes, a transfer matrix model[18,19] (including torsion) was used to calculate the frequencies of the same case. This model included 20 lumped masses, joined by massless uniform segments along the blade; a much more refined and time-consuming numerical model compared with the present method. Differences between the results of these two sets of calculations has been $<1\%$ and, in fact, at the scale of Fig. 2, both results coincide.

At zero δ_3, the first and second modes of vibration are the first and second flap modes, respectively, where the first is essentially rigid body flapping, a once-per-revolution mode, for zero offset. The lowest (cantilever) torsion mode frequency is the third mode shown. Thus, for zero δ_3, there is no coupling between flap and torsion. This coupling appears and grows as δ_3 is increased. Although the third, primarily torsion mode frequencies decrease somewhat at small values of δ_3, the major decreases occur in the region 60 deg $< \delta_3 <$ 90 deg. Large sharp changes of the second flap mode frequency also take place in the region 70 deg $< \delta_3 <$ 90 deg. In the case of the first mode, there are almost no changes up to $\delta_3 = 80$ deg, with such small changes as do take place occurring in the final 10 deg.

As a result of the flap-pitch coupling, the nature of the modes is changed by increasing δ_3. At $\delta_3 = 90$ deg, the first mode becomes the rigid body torsional rotation of a free/free rod without polar symmetry, thus having a slightly less than once-per-revolution natural frequency, caused by what is often called the tennis racquet effect. The second and third modes become the first and second flap modes, respectively, of a clamped/free blade. Although not presented in the figure, the first elastic torsional mode of a free/free blade so calculated agrees very well with transfer matrix and analytic calculations.

C. Case of a Fully Articulated Blade Having Linear Springs and Viscous Dampers About the Hinges

This example deals with a blade having orthogonal flap, lead-lag, and pitch hinges at its root, at zero offset relative to the shaft. The spring stiffness about the flap, lead-lag, and pitch hinges are k_β, k_ζ, and k_θ, respectively; the corresponding damping coefficients are C_β, C_ζ, and C_θ. It is assumed that for small vibrations about and undeformed state there is no coupling between motions about the hinges. The boundary conditions are then

$$v(x=0) = w(x=0) = 0 \quad (29a)$$

$$(EI_{\eta\eta})v_{e,xx}(x=0) - k_\zeta v_{,x}(x=0) - C_\zeta \dot{v}_{,x}(x=0) = 0 \quad (29b)$$

$$(EI_{\zeta\zeta})w_{e,xx}(x=0) - k_\beta w_{,x}(x=0) - C_\beta \dot{w}_{,x}(x=0) = 0 \quad (29c)$$

$$(GJ)\phi_{e,x}(x=0) - k_{\theta\phi}(x=0) - C_{\theta\dot{\phi}}(x=0) = 0 \quad (29d)$$

Based on these conditions, the matrix $[R1]$ of Eq. (2) [and Eq. (3b)] becomes

$$[R1] = \begin{bmatrix} \langle M1 \rangle \\ \langle M2 \rangle \\ \langle M3 \rangle \\ \langle M4 \rangle \\ \langle M5 \rangle \end{bmatrix} \quad (30)$$

Note that the indices, 7, 8, 9 have no sequential implications; they have been chosen simply to distinguish these row vectors from those with indices 3, 4, 5 in the previous section. All of the row vectors are of order N. $\langle M1 \rangle$ and $\langle M2 \rangle$ are defined by Eqs. (23a) and (23b). The rest are defined by the following equation:

$$\begin{bmatrix} \langle M7 \rangle \\ \langle M8 \rangle \\ \langle M9 \rangle \end{bmatrix} = [G1]\,[D1]^{-1}\,[D2] - [G2] \quad (31)$$

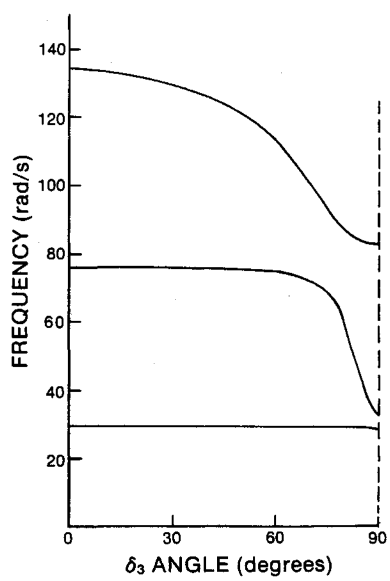

Fig. 2 Influence of δ_3 angle on the frequencies of the first three flap/torsion modes of vibration ($\Omega = 29.95$ rad/s).

The rectangular matrices $[G1]$ and $[G2]$ are of order $3xN_e$ and $3xN$, respectively.

$$[G1] = \begin{bmatrix} \langle g1v \rangle & & 0 \\ & \langle g1w \rangle & \\ 0 & & \langle g1\phi \rangle \end{bmatrix} \tag{32}$$

$$\langle g1v \rangle = (EI_{\eta\eta})\langle FV''_{e(1)}(x=0), \ldots, FV''_{e(j)}(x=0), \ldots, FV''_{e(Nve)}(x=0) \rangle \tag{33a}$$

$$\langle g1w \rangle = (EI_{\zeta\zeta})\langle FW''_{e(1)}(x=0), \ldots, FW''_{e(k)}(x=0), \ldots, FW''_{e(Nwe)}(x=0) \rangle \tag{33b}$$

$$\langle g1\phi \rangle = (GJ)\langle F\phi'_{e(1)}(x=0), \ldots, F\phi'_{e(l)}(x=0), \ldots, F\phi'_{e(N\phi e)}(x=0) \rangle \tag{33c}$$

The matrix $[G2]$ is also assembled of three row vectors (of orders N_v, N_w, and N_ϕ) as follows:

$$[G2] = \begin{bmatrix} \langle g2v \rangle & & 0 \\ & \langle g2w \rangle & \\ 0 & & \langle g2\phi \rangle \end{bmatrix} \tag{34}$$

where

$$\langle g2v \rangle = k_\zeta \langle 0, 1, 0, \ldots, 0 \rangle \tag{35a}$$

$$\langle g2w \rangle = k_\beta \langle 0, 1, 0, \ldots, 0 \rangle \tag{35b}$$

$$\langle g2\phi \rangle = k_\theta \langle 1, 0, \ldots, 0 \rangle \tag{35c}$$

Returning to the boundary conditions [Eqs. (29b–d)], we find that the matrix $[R2]$ in Eq. (2) [and Eq. (5b)] will be

$$[R2] = \begin{bmatrix} \langle g3v \rangle & & 0 \\ & \langle g3w \rangle & \\ 0 & & \langle g3\phi \rangle \end{bmatrix} \tag{36}$$

where $\langle g3v \rangle$, $\langle g3w \rangle$, and $\langle g3\phi \rangle$ are vectors of order N_v, N_w, and N_ϕ, respectively, defined as

$$\langle g3v \rangle = \langle 0, -C\zeta, 0, \ldots, 0 \rangle \tag{37a}$$

$$\langle g3w \rangle = \langle 0, -C_\beta, 0, \ldots, 0 \rangle \tag{37b}$$

$$\langle g3\phi \rangle = \langle -C_\theta, 0, \ldots, 0 \rangle \tag{37c}$$

Using Eqs. (25a–c) and (28), the natural frequencies and mode shapes are calculated. Figures 3a–c show the influences of root springs, k_β, k_ζ, and k_θ on the associated (uncoupled) frequencies without damping.

The influence of changing the flapping spring stiffness by even four orders of magnitude is shown in Fig. 3a to be relatively small. Resultant flapping restoring forces are dominated by centrifugal effects, and, thus, the difference between free hinges ($k_\beta = 0$) and hingeless ($k_\beta \to \infty$) is small. The figure also presents a comparison between the present method and the results of a transfer matrix calculation. The two first modes agree so well as to virtually coincide. There are small differences in the computed frequencies of the third mode that probably would disappear with a larger number of flapping generalized coordinates.

Relatively large influences of root springs are shown in Figs. 3b and 3c for lead-lag and torsional modes. For zero spring stiffness, the frequency of the first lead-lag mode tends to zero. Without such springs or lag-hinge offsets, of course, rotational torque cannot be applied; such a case, then, is of limited interest. There is also very good agreement in Figs. 3b and 3c between the results of the present method and transfer matrix calculations. In fact, the two torsional modes and the first lead-lag mode practically coincide, whereas there are small differences in the case of the second lead-lag mode, probably reflecting the limited number of elastic lead-lag bending modes used in the analysis.

A point of interest usually considered in modal analyses is the accuracy with which natural boundary conditions can, in fact, be achieved. In the method of this paper, Eqs. (29b–d) ensure that such criteria are imposed explicitly. It is well known that the usual energy approaches do not require that such conditions be satisfied; mode shapes to be chosen for the generalized coordinates, in contrast to those assumed in Eqs. (19a–e), usually are recommended as those that individually satisfy boundary conditions. In order to examine this point, calculations for the case $k\beta = 0$ have also been carried out in which the natural boundary conditions were not imposed directly [i.e., eliminating Eq. (29c) and the corresponding Lagrange multiplier from the calculation]. Frequencies calculated by either including Eq. (29c) or eliminating it were practically the same. The mode shapes obtained from these two calculations also agreed very well. The flapwise bending moment distributions calculated for the first, primarily elastic flap-bending mode (the second flap mode) are compared in Fig. 4. It is seen that the agreement between both calculations is again very good, except for the root region (i.e., within $< 10\%$ of the blade length from the root). With all conditions imposed, the root bending moment became zero as required; the less complete case shows a small nonzero value for moment at the root.

In considering Fig. 4, it is noteworthy that a typical simply supported/free bending mode shape (which is not shown here) and the associated moment distribution are obtained with this excellent accuracy as a result of superposing only five clamped/free modes! The ability of the model to yield such high-quality bending moments is a strong indication of the usefulness of the present approach.

D. Comparisons with Analytic Solutions

All of the numerical results presented to this point have dealt with the case of zero damping. Thus, the boundary conditions did not include rate influence at the root. To assess the accuracy of results obtained for a case where such damping exists, an arrangement that includes both pitch spring and pitch damping at the root of a nonrotating blade was considered. The results of the present method were then compared with those of an exact analytical solution. The latter were obtained by deriving a characteristic equation reflecting impositon of exact boundary conditions for each end of a uniform torsion bar. Its solution yields the natural frequencies and damping characteristics in the form of complex eigenvalues.[20] The solution technique treats the characteristic equation in its real and imaginary parts, each of which must be satisfied simulaneously. These equations are algebraically nonlinear, and the secant method[21] was used to solve them.

Table 1 lists two sets of complex eigenvalues for the first and second torsional modes (real and imaginary parts) for six different values of damping coefficient C_θ for a constant value of the root torsional spring stiffness $k_\theta = 67787$ N-m/rad. One set results from application of the present method; the other set from the exact analytical calculations.

Agreement between the two sets of eigenvalues for the first torsional mode is excellent for all of the damping values. Slightly larger differences appear in the case of the second torsional mode, but the agreement between present method and exact calculation results are still very good.

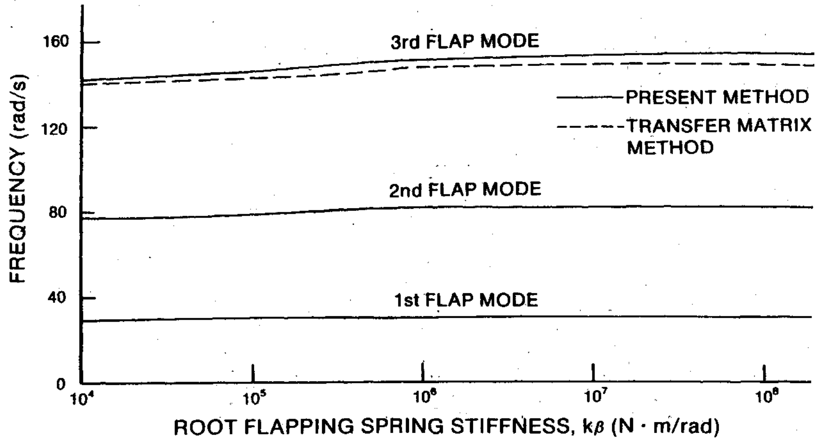

Fig. 3a Influence of a flapping root spring on the first three flap frequencies (zero damping at the root).

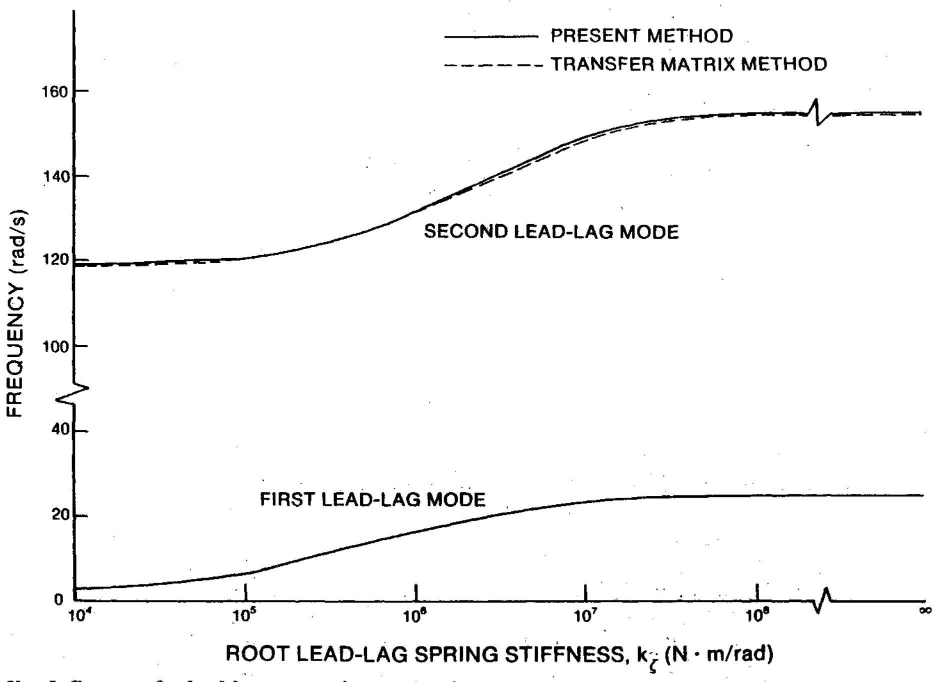

Fig. 3b Influence of a lead-lag root spring on the first two lead-lag frequencies (zero damping at the root).

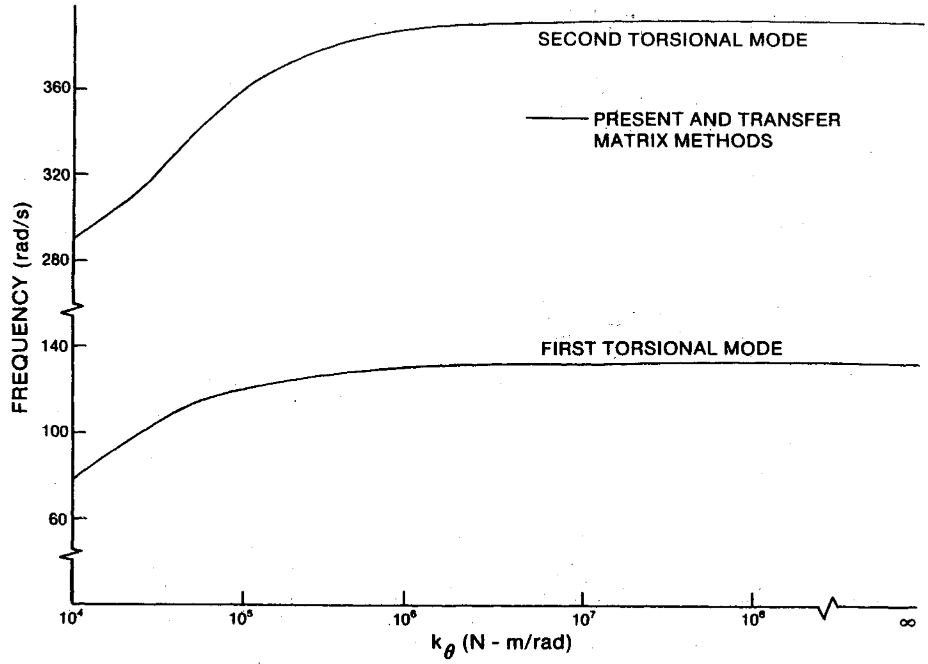

Fig. 3c Influence of a torsional root spring on the first two torsional frequencies (zero damping at the root).

Table 1 Comparison between the eigenvalues (λ) of the first and second torsional modes of a nonrotating blade having a pitch spring (k_θ) and viscous damper (C_θ) at the root (in all cases $k_\theta = 67787$ N-m/rad)

Root damping coefficient C_θ N-m s/rad	Present method				"Exact" analytical calculations			
	First mode		Second mode		First mode		Second Mode	
	Real	Imag.	Real	Imag.	Real	Imag.	Real	Imag.
0.01	−0.234E−03	114.8	−0.168E−2	348.6	−0.234E−03	114.8	−0.169E−2	348.1
0.1	−0.234E−02	114.8	−0.168E−1	348.6	−0.234E−02	114.8	−0.169E−1	348.1
1.0	−0.234E−01	114.8	−0.168	348.6	−0.234E−01	114.8	−0.169	348.1
10^2	−2.308	115.1	−15.55	353.6	−2.307	115.1	−15.77	353.2
10^3	−7.616	126.7	−9.399	391.1	−7.616	126.7	−9.399	391.0
10^4	−0.9586	130.9	−0.9605	392.7	−0.9585	130.9	−0.9605	392.7

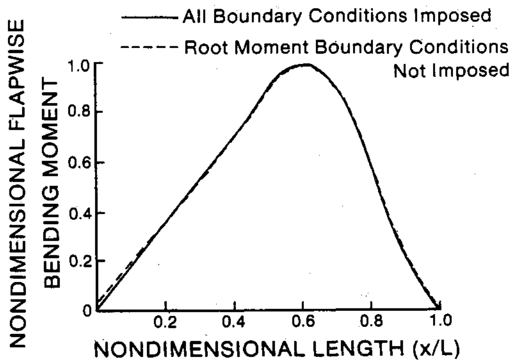

Fig. 4 Flapwise bending moment distribution in the second flap mode.

V. Conclusions

A recently derived analysis method, combining a principal curvature transformation, velocity component transformation, and generalized coordinates techniques, was extended using the Lagrange multiplier approach to yield a unified model capable of dealing with virtually all possible auxiliary conditions as they may be applied in blade design.

This use of the method of Lagrange multipliers has been shown to be a convenient way of dealing with auxiliary conditions in the analysis of blade dynamics. Application of this method increases the number of unknowns by the number of auxiliary conditions, but the influence of these conditions is confined in the mathematical sense to limited components of the computational model. Thus, it is relatively easy to examine the effect of additional auxiliary conditions or of variations in the parameters describing conditions that are already represented.

By choosing a specific set of generalized coordinates, namely, rigid body displacements and modes cantilevered at the root, this model becomes particularly simple and efficient for rotor blade design where it is necessary to evaluate the effect of root restraints. Despite the fact that none of these shape functions may individually satisfy boundary conditions at the root, the method, using only a small number of generalized coordinates, provides results that agree very well with those obtained from transfer matrix calculations. The sample cases presented here include δ_3 hinges and root hinges incorporating linear rotational springs and viscous dampers.

Requiring that moment boundary conditions be satisfied does not seem to have a major influence on natural frequencies or mode shapes. But, on the other hand, this may be important when bending moment distributions are of interest, and some differences were appreciable in such comparisons.

In sum, it seems that the method of Lagrange multipliers combined with a generalized coordinates approach offers an efficient tool for dealing with complicated auxiliary conditions of all kinds. Such should be true for auxiliary conditions imposed at any point on the blade and for nonlinear as well as linear cases, although only linear, root conditions have been examined here.

Acknowledgments

The research was supported primarily by the Army Research Office through the Rotorcraft Technology Center at Rensselaer Polytechnic Institute under Contracts DAAG-29-82-K-0093 and DAAL03-88-C-0004. Robert Singleton and Gary Anderson were Contract Monitors.

References

[1]Johnson, W., *Helicopter Theory*, Princeton Univ. Press, Princeton, NJ, 1980.

[2]Rosen, A., and Rand, O., "A General Model of Helicopter Blade Dynamics," *Vertica*, Vol. 9, No. 1, 1985, pp. 35–50.

[3]Stroub, R. H., "Performance Improvements with the Free-Tip Rotor," *Proceedings of the American Helicopter Society National Specialists' Meeting, Rotor System Design,* Philadelphia, PA, Oct. 1980, pp. I 4.1–I 4.7.

[4]Stroub, R. H., Young, L. A., Keys, C., and Cawthorne, M., "Free-Tip-Rotor Wind-Tunnel Test Results," *Proceedings of the 41st Annual National Forum of the American Helicopter Society*, Ft. Worth, TX, May 1985, pp. 387–411.

[5]Weller, W. H., and Lee, B. L., "Wind-Tunnel Tests of Wide-Chord Teetering Rotors With and Without Outboard Flapping Hinges," NASA TP-1046, Nov. 1977.

[6]Griffiths, J. B., *The Theory of Classical Dynamics*, Cambridge Univ. Press, New York, 1985.

[7]Nikravesh, P. E., *Computer-Aided Analysis of Mechanical Systems*, Prentice-Hall, Englewood Cliffs, NJ, 1988.

[8]D'Souza, A. F., and Grag, V. K., *Advanced Dynamics, Modeling and Analysis*, Prentice-Hall, Englewood Cliffs, NJ, 1984.

[9]Rosenberg, R. M., *Analytical Dynamics of Discrete Systems*, Plenum, New York, 1980.

[10]Hsu, J. C., and Meyer, A. V., *Modern Control, Principles and Applications*, McGraw-Hill, New York, 1968, Chap. 13.

[11]Rosen, A., Loewy, R. G., and Mathew, M. B., "Nonlinear Analysis of Pretwisted Rods Using Principal Curvature Transformation, Part I: Theoretical Derivation," *AIAA Journal*, Vol. 25, No. 3, 1987, pp. 470–478.

[12]Rosen, A., Loewy, R. G., and Mathew, M. B., "Nonlinear Analysis of Pretwisted Rods Using Principal Curvature Transformation," Part II: Numerical Results," *AIAA Journal*, Vol. 25, No. 4, 1987, pp. 598–604.

[13]Rosen, A., Loewy, R. G., and Mathew, M. B., "Nonlinear Dynamics of Slender Rods," *AIAA Journal*, Vol. 25, No. 4, 1987, pp. 611-619.

[14]Loewy, R. G., Rosen, A., and Mathew, M. B., "Application of the Principal Curvature Transformation to Nonlinear Rotor Blade Analysis," *Vertica*, Vol. 11, No. 1/2, 1987, pp. 263–296.

[15]Rosen, A., Loewy, R. G., and Mathew, M. B., "A Study of the Influence of Predeformations on the Vibrations of Blades," *Journal of Sound and Vibration* (to be published).

[16]Bisplinghoff, R. L., Ashley, H., and Halfman, R. L., *Aeroelasticity*, Addison-Wesley, New York, 1957.

[17]Washizu, K., *Variational Methods in Elasticity and Plasticity*, 1st ed., Pergamon, New York, 1968, Chap. 5.

[18]Isakson, G., and Eisley, J. G., "Natural Frequencies in Bending of Twisted Rotating and Nonrotating Blades," NASA TN-D-371, March 1960.

[19]Isakson, G., and Eisley, J. G., "Natural Frequencies in Coupled Bending and Torsion of Twisted Rotating and Nonrotating Blades," NASA CR-65, July 1964.

[20]Thomson, W. T., *Vibration Theory and Applications*, Prentice-Hall, Englewood Cliffs, NJ, 1965, Chap. 8.

[21]Wolfe, P., "The Secant Method for Simultaneous Non-Linear Equations," *Communications of the ACM*, Vol. 2, No. 12, 1959, pp. 12,13.